

# TEMPERATURE PROFILE ESTIMATION WITH SMART TEXTILES

I. Locher

*Electronics Laboratory - Wearable Computing Lab, Department of Information Technology and Electrical Engineering, ETH Zurich, Switzerland*

*ilocher@ife.ee.ethz.ch*

T. Kirstein & G. Tröster

*Electronics Laboratory - Wearable Computing Lab, Department of Information Technology and Electrical Engineering, ETH Zurich, Switzerland*

## ABSTRACT

*Current trends in e-textiles and smart fabrics try to find a symbiosis of electronics and clothing. Augmenting a fabric with an intrinsic sensing function is an elegant way to measure the environment. This approach supports the idea of a smooth combination of the two worlds of electronics and clothing. Our hybrid fabric senses temperature and estimates the temperature profile along the surface. We explain the measurement principle and show how a measurement accuracy of 0.5K with a 10cm long piece of fabric can be achieved. We also point out potential applications of our fabric temperature sensor.*

## 1 INTRODUCTION

The realization of our vision of continuous healthcare and assistance during daily life necessitates an unobtrusive embedding of sensors and electronics in our outfit without affecting wearing comfort. Sensors are distributed all over the body, often requiring direct contact to the skin. Smart fabrics with intrinsic sensing functionality offer an optimal solution to satisfy these requirements. Moreover, anything that utilizes fabrics from clothing until car interior could be made 'smart'.

In this paper, we present a smart fabric system with temperature sensing capability. The goal is to achieve a measurement accuracy of 0.5 Kelvin over a temperature range of 10°C to 60°C that is comparable to commercial products such as thermistors (e.g. Pt100) and thermocouples. The woven structure of the hybrid fabric itself represents an array of temperature sensors that can be utilized to measure the temperature profile of a surface. To our knowledge, such a smooth embedding of temperature sensing capability into a fabric is novel.

Our hybrid fabric is not only capable of temperature sensing, but also for signal transmission. Currently, many research labs concentrate on the side of signal transmission [1],[2],[3],[4].

Temperature measurement is one option, but fabrics have the capacity to integrate other sensing functionality. Lorussi *et al.* [5] work on fabric-based strain sensors in order to track body postures. Companies such as Softswitch, Eleksen and ITP investigate in fabric pressure sensors.

## 2 MEASUREMENT CONCEPT

In this section, we briefly present the physical principle for our temperature measurements. In our method, we utilize the temperature dependence of the electrical resistance of metals according to (1).

$$R_{wire} = \rho_{metal}(1 + \alpha_{metal} \cdot \Delta T) \frac{l_{wire}}{A_{wire}} \quad [\Omega] \quad (1)$$

$\rho_{metal}$  is the specific resistance and  $\alpha_{metal}$  is the temperature coefficient.  $A_{wire}$  denotes the cross-section area and  $l_{wire}$  the length of the metal wire.  $\alpha_{metal}$  is similar for all metals and features about  $0.4\%/K$  for copper. The length elongation as well as the quadratic coefficient of resistance change due to temperature variations are negligibly small for our intended measurement range from  $0^\circ C$  to  $60^\circ C$ . We utilize thin copper wires with about  $14.16\Omega/m$  at  $20^\circ C$  for our measurements. The wires are embedded in a fabric as will be seen in section 3. The intended temperature profile estimation requires a grid of sensors. In a demo application, we applied a  $10 \times 10 cm^2$  hybrid fabric patch as measurement array with a spatial resolution of  $1 cm$ .

### 3 HYBRID FABRIC SENSOR

The hybrid fabric is fabricated by Sefar Inc. It consists of woven polyester yarn (PET) with diameter of  $42\mu m$  and copper alloy wires with diameter  $50 \pm 8\mu m$ . The hybrid fabric with a mesh opening of  $95 \pm 10\mu m$  and an opening area of 44% is shown in Figure 1. Each copper wire itself is coating with a polyurethane varnish as electrical insulation. The copper wire grid in the textile features a spacing of  $0.57 mm$  (mesh count in warp and in weft is  $17.5 cm^{-1}$ ). The combination of PET yarn and copper wires requires a special weaving technology, which includes two yarn systems in warp and weft direction (3 PET wires and 1 copper wire) with separate tensioning systems. The hybrid fabric with its weight of  $74 g/m^2$  is positioned as interlining. Its application field is therefore very versatile. The fabric represents a compromise between preserving textile properties and copper wire density. To our knowledge, such a precise hybrid fabric consisting of PET yarn and copper wire is new to the market.

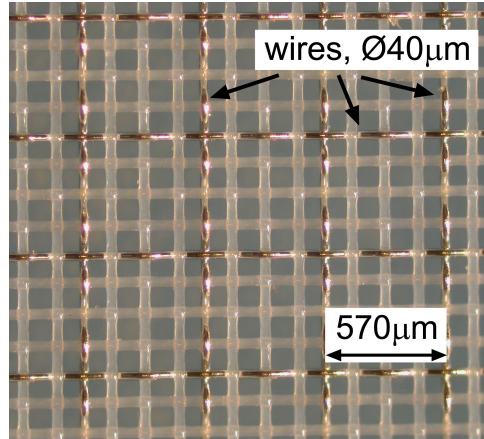


**Figure 1: Fabric with embedded copper wires as temperature sensors (Sefar Inc.)**

Due to the low mass of a wire ( $123 dtex = 12.3 \mu g/m$ ) and the high thermal conductivity of copper, such a temperature sensor reacts quickly towards thermal changes.

### 4 ELECTRONIC MEASUREMENT CIRCUIT

Since the resistance of the thin copper wire as well as its temperature coefficient  $\alpha_{Cu}$  are small, the electronics must measure very precisely to achieve the targeted accuracy of  $0.5 K$ . Thus,

we utilize the 4-wire resistance measurement principle. Secondly, we propose a new difference measurement method in order to eliminate circuit offsets.

#### 4.1 Measurement Principle

The principle measurement circuit is shown in Figure 2. By imposing a constant current through the copper wire and measuring the resulting voltage drop, the wire resistance can be extracted and therefore, the temperature according to (2).  $R_{wire0}$  defines the reference resistance of the wire at a certain temperature, i.e.  $20^{\circ}C$ .

A constant current through the wire is ensured by the operational amplifier (OA), which regulates its output such that its (+) and (-) inputs feature the same potential. The instrumental amplifier (IA) boosts the differential signal such that a measurement resolution of  $0.4K/LSB$  is achieved for our demonstrator. The lowpass filter reduces noise and avoids aliasing by limiting the signal bandwidth to  $f_c = 160Hz$ . This bandwidth is a compromise between noise reduction and measurement speed. The analog-to-digital converter features a resolution of  $12Bits$ , which translates to a LSB (least significant bit) of  $0.5mV$  using a reference voltage of  $2.048V$ .  $R_2$  can be switched to the circuit that allows applying different currents through the copper wire. This procedure further improves measurement accuracy.

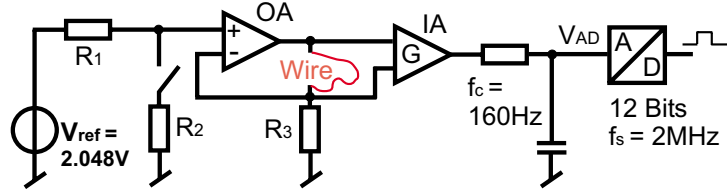


**Figure 2: Temperature Measurement Principle**

$$\Delta T = \left( \frac{R_{wire}}{R_{wire0}} - 1 \right) \cdot \frac{1}{\alpha_{Cu}} \quad [Kelvin] \quad (2)$$

Formula (3) gives the wire resistance in relation to the measured voltages  $V_{AD_h}$  and  $V_{AD_l}$  at the analog-to-digital converter. The two voltages correspond to the two currents that are generated by switching  $R_2$  on and off the circuit. Due to subtraction of the voltages, constant circuit offsets (e.g. amplifier offsets) are eliminated.

Putting (3) into (2), the constants  $R_1 - R_3$ ,  $G$  and  $V_{ref}$  cancel out leading to formula (4). As a result, the accuracies of these constants become unimportant when using a reference wire resistance  $R_{wire0}$  determined by calibration. In fact, the voltages in formula (4) can directly be replaced with the  $bits_x$  correspond to the binary values of the analog-to-digital converter. This then leads to formula (5).

$$R_{wire} = \frac{R_3}{G} \cdot \frac{R_1 + R_2}{R_2} \cdot \frac{V_{AD_h} - V_{AD_l}}{V_{ref}} \quad [\Omega] \quad (3)$$

$$T = \left( \frac{V_{AD_h} - V_{AD_l}}{V_{AD_{refh}} - V_{AD_{refl}}} - 1 \right) \frac{1}{\alpha_{Cu}} + T_0 \quad [^{\circ}C] \quad (4)$$

$$T = \left( \frac{bits_h - bits_l}{bits_{refh} - bits_{refl}} - 1 \right) \frac{1}{\alpha_{Cu}} + T_0 \quad [^{\circ}C] \quad (5)$$

$R_{wire0}$ , i.e.  $bits_{refh}$  and  $bits_{refl}$ , can be determined with a single point calibration. However,  $\alpha_{Cu}$  determines the slope of the resistance change by temperature. The value of  $\alpha_{Cu}$  is not precisely known since literature gives values ranging from  $0.0039K^{-1}$  to  $0.00404K^{-1}$ . Secondly, the wires in our fabric consist of a copper alloy whose  $\alpha$  differ from a pure copper wire. Therefore, a 2-point calibration is necessary at least.

#### 4.2 Theoretical Temperature Accuracy

The total measurement tolerance depends on different factors. On the one hand, accuracy improves the longer a measurement wire within the fabric is. A longer wire directly corresponds to a higher resistance. On the other hand, location information about temperature changes decreases the longer a wire is. For instance, a temperature change could be spread along the entire wire as well as just locally at a single point. This behavior resembles the uncertainty principle.

Secondly, all measurements are noisy up to the bandwidth of  $160Hz$  and all electronic components are temperature dependent as well. We model our measurement system including parasitics for a worst case scenario the following way (6)

$$V_{AD} = f(T_{wire}) + V_{ofs} + V_{noise} + V_{drift} + V_{tol} \quad [V] \quad (6)$$

Whereas the circuit offsets  $V_{ofs}$  are cancelled by the difference measurement described in section 4.1, the circuit noise  $V_{noise}$  (thermal noise) can statically be reduces by multiple measurements  $N$  with an accuracy improvement following the  $1/\sqrt{N}$ -law. The reference voltage source  $V_{ref}$ , the OA and the IA identify the biggest noise sources, though they are rather constant over temperature.  $V_{drift}$  describes the temperature dependence of the electronic circuit whereas  $R_1 - R_3$  feature the biggest influence with a datasheet value of  $15ppm/K$ . Thirdly, the analog-to-digital converter with its accuracy of  $0.19K/LSB$  according to the datasheet introduces a quantization noise of about  $0.22K$ .

Figure 3 depicts the different inaccuracy sources of the circuit as a function of temperature. Circuit noise contributes most to the error, but it can be minimized by multiple measurements. Therefore, an accuracy of about  $0.5K$  can be achieved with single measurement.

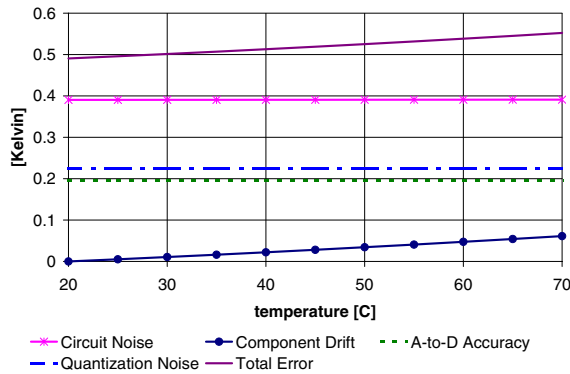


**Figure 3: Contributions to Temperature Measurement Inaccuracy**

## 5 TEMPERATURE MEASUREMENTS

In this section, measurement verification of our demonstrator is described. Note that our reference thermometer (Fluke DMM with thermocouple) itself has an accuracy of only  $\pm 1\%$  ( $+3^\circ C$ ). Figure 4 shows the temperature linearity neglecting the tolerances of the reference thermometer.

Since we do not know  $\alpha_{metal}$  exactly, the slope of the measured curve with an assumed  $\alpha = 0.00404K^{-1}$  (thin solid line in the figure) is too flat. However, we approximated the true  $\alpha_{metal}$  with the given measurements by means of formula (7) resulting in an  $\alpha_{true} = 0.0035K^{-1}$ . The corresponding  $\alpha$ -compensated curve is depicted as thick solid line in the figure. The measurement points of the fitted curve feature a standard deviation of  $\sigma_e = 1.2K$  to a ideal curve (straight line).

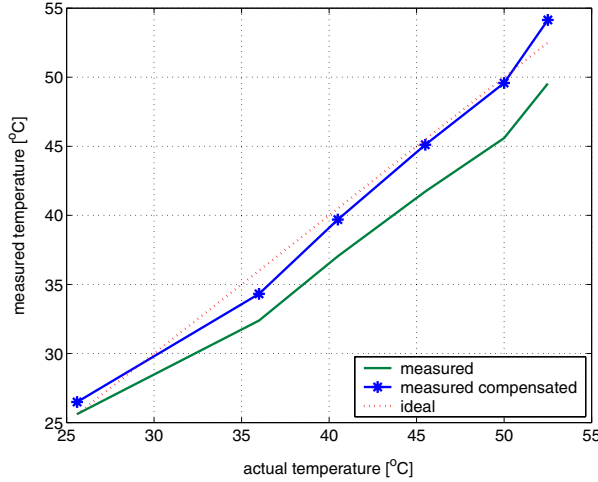


**Figure 4: Temperature Measurement Linearity**

$$\alpha_{true} = \alpha_{Cu} \frac{(T_{meas} - T_0)^T (T_{meas} - T_0)}{(T_{act} - T_0)^T (T_{meas} - T_0)} \quad [K^{-1}] \quad (7)$$

The approximation (7) was computed using the least mean square error approach shown in formula (8).

$$\frac{\partial}{\partial \alpha_{true}} \sum_i [T_{act_i} - T_0 - (T_{meas_i} - T_0) \frac{\alpha_{Cu}}{\alpha_{true}}]^2 = 0 \quad (8)$$

### 5.1 Temperature Measurement Accuracy

In order to determine the measurement accuracy and repeatability, we repeatedly measured the same temperature (e.g. 500 times) using a climate chamber. Thus, we achieved a small standard deviation of  $\sigma = 0.39K$  at a temperature of about  $50^\circ C$ . The standard deviation behaved similarly for different temperatures. The temperature distribution is depicted in Figure 5. The measured values indicate better performance than the computed worst case scenario shown in section 4.2.

### 5.2 Surface Temperature Profile

The grid of copper wires in the hybrid fabric (section 3) allows measurement of temperature along a surface. For our demonstrator, we utilized a  $10 \times 10 cm^2$  hybrid fabric patch as tempera-

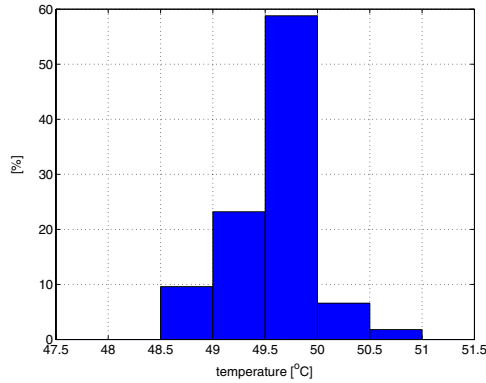


**Figure 5: Measurement Distribution over 500 Iterations at 50°C**

ture sensor array. A principle schematic is given in Figure 6. Due to the wire topology, location information of "hot spots" can be extracted by measuring wire resistance in x- and y-direction.

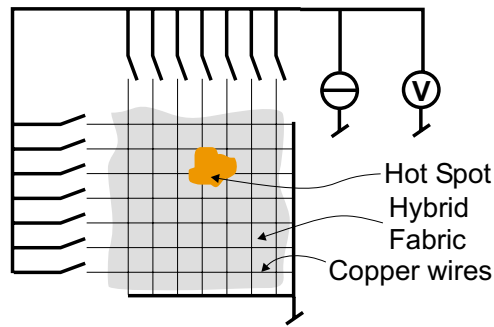


**Figure 6: Temperature Measurement Array**

Instantly, such a fabric seems to be attractive to measure temperature distribution across a surface. However, a measurement returns an averaged temperature along the wire whereby "hot spots" gets smeared out over the entire wire length. From a mathematical point of view, the system is under-determined since we only have  $2N$  measurements in a  $N \times N$  grid with  $N^2$  cross-points for temperature measurement. This fact leads to spatial ambiguity. Unless all the "hot spots" are aligned in a row or a column, additional virtual "hot spots" occur. For example, the measurement of two actual "hot spots" on the fabric result in detection of two additional virtual "hot spots" as can be seen in Figure 7. Three actual "hot spots" result in an additional 6 virtual "hot spots", etc.

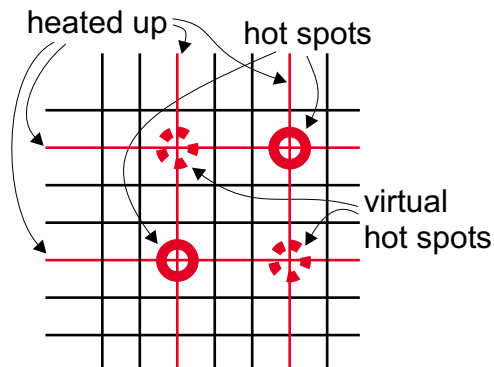


**Figure 7: Measurement Ambiguity due to Grid Structure**

A restriction to single "hot spot" detection relaxes the problem such that no ambiguity occurs. The temperature distribution estimation of such a single "hot spot" is shown in Figure 8, where a finger touched the fabric in the rear corner. The estimated distribution of the temperatures is computed by taking the outer product of the temperatures along the row and column wires according to (9)

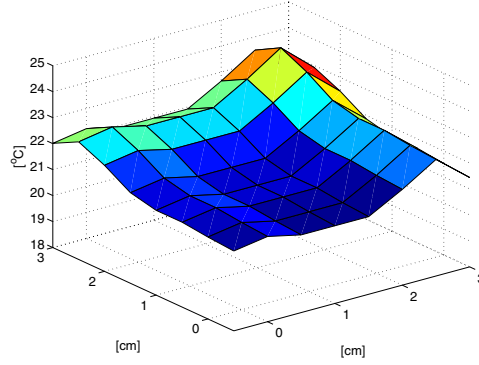


**Figure 8: Temperature Distribution along Fabric**

$$T_{est} = \sqrt{T_{row} \cdot T_{col}^T} \quad [^{\circ}C] \quad (9)$$

### 5.3 Measurement Ambiguity Avoidance

By shrinking the patches to a size where ambiguity does not matter anymore, e.g. an area of  $2 \times 2 \text{ cm}^2$ , and by applying several of these patches in an array, overall ambiguity can be eliminated. Such patches can be designed by fabric interconnection techniques as described in [1]. An array of patches is depicted in Figure 9. The connects guarantee a longer wire such that the targeted temperature resolution can be achieved.

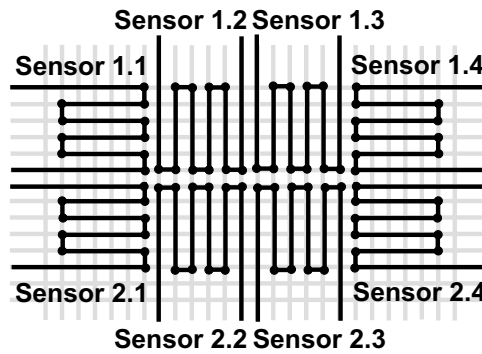


**Figure 9: Array of Temperature Measurement Patches**

## 6 CONCLUSION

In this paper, we have presented a fabric temperature sensor with an accuracy of about  $1K$  when using a 2-point calibration. This accuracy can further be improved to  $0.5K$  by recording the entire curve over the temperature range such that non-linearity can be compensated. Additionally, more sophisticated electronics with temperature compensation and less noisy components advances performance as well.

Secondly, we have shown how spatial resolution can be improved without ambiguity. Such fabric temperature sensors can smoothly be integrated into clothing providing a platform for temperature profile measurement along the human body. Many applications are feasible, e.g. monitoring of temperature to which firefighters are exposed during their missions. Other applications could lie in the medical field. A new idea is use our sensor array to protocol the food intake over the day by measuring skin temperature close to the liver [6], [7].

The sensors do not necessarily need to be integrated into clothing, e.g. a car seat equipped with these sensors could measure skin temperature as well.

## REFERENCES

- [1] Ivo Locher, Tünde Kirstein, and Gerhard Tröster. Routing methods adapted to e-textiles. In *Proc. 37th International Symposium on Microelectronics (IMAPS 2004)*, November 2004.
- [2] e-textiles. Virginia Tech. <http://www.ccm.ece.vt.edu/etextiles>.
- [3] S. Jung, Ch. Lauterbach, M. Strasser, and W. Weber. Enabling technologies for disappearing electronics in smart textiles. In *IEEE International Solid-State Circuits Conference*, San Francisco, CA, February 9-13 2003.
- [4] Christine Kallmayer, Torsten Linz, Rolf Aschenbrenner, and Herbert Reichl. System integration technologies for smart textiles. *mst news*, 2:42–43, 2005.
- [5] F. Lorussi, W. Rocchia, E. P. Scilingo, A. Tognetti, and D. De Rossi. Wearable, redundant fabric-based sensor arrays for reconstruction of body segment posture. *IEEE Sensors Journal*, 4(6):807–818, December 2004.
- [6] M. S. Westerterp-Plantenga, L. Wouters, and F. Ten Hoor. Deceleration in cumulative food intake curves, changes in body temperature and diet-induced thermogenesis. *Physiology & Behavior*, 48:831–836, 1990.
- [7] Jan De Vries, Jan H. Strubbe, Wic C. Wildering, Jan A. Gorter, and Ab J. A. Prins. Patterns of body temperature during feeding in rats under varying ambient temperatures. *Physiology & Behavior*, 53:229–235, 1993.